Marder, E., Gallen, S.F., and Pazzaglia, F.J., 2023, Late Cenozoic deformation in the U.S. southern Colorado Front Range revealed by river profile analysis and fluvial terraces: GSA Bulletin, https://doi.org/10.1130/B36440.1.

Supplemental Material

Text S1. Methods additional information.

Figure S1. Slope-Drainage Area plot for 100 m streamwise distance increments along the eastern Rockies drainage network (grey points) overlain by log-binned averages of the raw data (purple squares).

Figure S2. Result from the variance minimization method used to calculate $\theta_{ref}=0.41$ for the eastern Rockies drainage network.

Figure S3. Flexural response of the Arkansas River valley across the western High Plains under T_e = 5, 10, and 15 km.

Table S1. Summary of terrace strath elevations and alluvial fill thicknesses as measured in the field.

Supplementary Materials

Contents of this file

- Text S1: Methods additional information
- Figures and tables captions
- Figures S1 to S3
- Table S1

Text S1: Methods additional information

Digital topographic analysis

We delineated the eastern Rockies fluvial network based on linear relationships between the log of drainage slope, S, and the log of upstream drainage area, A (Fig. S1; Snyder, 2000; Wobus et al., 2006; Kirby and Whipple, 2012). This analysis suggests that the transition between fluvially- and colluvially-dominate channels occur at a drainage area of ~3e^{4} m^{2} (Fig. S1). To ensure that we only work in the fluvially-dominated portion of the channels and follow the detachment-limited stream power incision model assumptions (i.e., bedrock channels are not affected by hillslope and sediment processes; e.g., Snyder, 2000; Kirby and Whipple, 2012), we conservatively used a drainage area threshold ≥ 10^{6} m^{2} to define drainage networks in the eastern Rockies. We calculated the regional-scale concavity, θ_{ref}, in the eastern Rockies using the variance minimization function 'mnoptimvar' (Fig. S2) in TopoToolbox. We used this empirically-derived θ_{ref} to calculate χ across the eastern Rockies drainage network, evaluate k_{sn} for binned segments along it, and interpolate k_{sn} for the entire eastern Rockies region (Fig. 3C, main text).

River profile analysis

Basin-wide linear inversion

We evaluated the relative base level fall history of each basin using a linear inversion approach. We discretized equation 7 (see main text) to solve for the average basin k_{sn} for a discrete $\Delta\chi$ interval, such that:

$$z_j = 1k_{sn_1}\Delta\chi_1 + 2k_{sn_2}\Delta\chi_2 + \cdots + qk_{sn_{j-2}}\Delta\chi_{j-2} + qk_{sn_{j-1}}\Delta\chi_{j-1} \qquad \text{(S1).}$$

Equation DR1 can be written as a matrix forward problem:

$$Ak_{sn} = z \qquad \text{(S2),}$$

where A is an n by q sized matrix, where n is the number of stream nodes, and q is the number of discrete domains:

$$A = \begin{bmatrix} \Delta\chi_1 & \cdots & q\Delta\chi_1 \\ \vdots & \ddots & \vdots \\ \Delta\chi_n & \cdots & q\Delta\chi_n \end{bmatrix} \quad \text{(S3).}$$

The Tikhonov regularization for Equation S2 is:

$$k_{sn} = {k_{sn}}^{pri} + (A^T A + \Gamma^2 I)^{-1} A^T (z - A{k_{sn}}^{pri}) \quad \text{(S4),}$$

where ${k_{sn}}^{pri}$ is a prior guess for k_{sn}, Γ is a dampening coefficient that determines the smoothness imposed on the solution, and I is the $q\ X\ q$ identity matrix. We used these equations to conduct a linear inversion of χ-elevation data for each of the basins in the eastern Rockies and compared them with the tributary trunk channel χ-plots and knickpoints (Fig. 4, main text). Under the assumption that K is spatially and temporally uniform and rock uplift rate is spatially uniform, changes in base level fall rate will translate upstream at the same rate in χ-transformed distance space. In this case, the results of linear inversion of χ-elevation data can be interpreted as a test for genetically-related knickpoints, analogous to applications of the knickpoint celerity model (e.g., Crosby and Whipple, 2006; Berlin and Anderson, 2007; Gallen et al., 2013; Miller et al., 2013). However, in the case of the linear inversion, all data in the fluvial network is analyzed rather than just hand-selected knickpoint data, and related knickpoints can be identified as spikes or steps in χ-binned k_{sn} plots. If it is assumed that the slope exponent in the stream power model, n, is equal to 1, this analysis reflects the relative history of base level fall assuming block uplift (cf. Goren et al., 2014). If K can be calibrated, the χ-binned k_{sn} plots can be converted to base level fall or rock uplift rate histories (e.g., Goren et al., 2014; Gallen, 2018).

Terrace analysis

To get a first identification of the presented surfaces in the western High Plains, we conducted 28 cross-sections across the Arkansas River Valley at 1 km intervals from Canon City, CO downstream to Pueblo, CO using Google Earth imagery. We measured 45 terrace strath elevations and alluvial fills above these straths using a TruPulse 360 Rangefinder in the field (Table S1). We verified the downstream terrace correlations by subdividing the LiDAR elevation data to equal increments of 10 m of elevation difference from the modern Arkansas River. We refined our terrace correlations by conducting a LiDAR hypsometry (Fig. 8, main text). For the hypsometry, we first removed "non-flat" areas in the LiDAR data using slope and curvature thresholds of 5° and ± 0.005, respectively, as well as mapped Holocene terraces along the Arkansas valley (Fig. 8, main text). We projected the mapped treads polygon edges to the Arkansas River Valley to evaluate estimated total incisions for each point from the modern Arkansas River.

Flexural Analysis

We conducted a 2D flexural response model to differential erosion beneath the estimated Rocky Flats (~1.3-2 Ma) paleo-surface along the western High Plains (Figs. 9, main text; S3). For the flexural model, we used a continuous two-dimensional elastic layer over an inviscid half-space (Watts, 2001):

$$D\frac{d^4w}{dx^4} + (\rho_m - \rho_c)gw = q \quad \text{(S5)}$$

$$D = \frac{ET_e^{\ 3}}{(1-v)^2} \quad \text{(S6).}$$

where D is the lithospheric rigidity, w is the vertical deflection of the plate, ρ_m is the mantle density, ρ_c, is the crust/infill density, g, is the acceleration due to gravity (9.81 m s^{-2}), q, is the applied surface load based on the inferred eroded volume from the paleo-surface of the Rocky Flats, T_e, is the effective elastic thickness of the lithosphere, E, is the Young's modulus, and v, is the Poisson's ratio. To calculate the flexural deflection, w, we applied elastic thicknesses, $T_e = 5 - 15\ km$; mantle density, $\rho_m = 3300\ kg/m^3$; crust/infill density, $\rho_c = 2500\ kg/m^3$; Young's modulus, $E = 10^{11}\ Pa$; and Poisson's ratio, $v = 0.25$, following previous geophysical studies in the region (Lazear et al., 2013; Hansen et al., 2013). All calculations assumed spatially uniform lithospheric rigidity and were solved in the spectral domain. Forward and inverse fast Fourier transforms were used to move between the spatial and spectral domains and generate maps of two-dimensional surface deflections (Fig. S3).

Figures and tables captions

Figure S1: Slope-Drainage Area plot for 100 m streamwise distance increments along the eastern Rockies drainage network (grey points) overlain by log-binned averages of the raw data (purple squares). A transition from colluvial to a fluvial regime is noticed at drainage areas of ~3e^4 m^2. In this study, only basins that drain > 1e6 m^2 were analyzed. Also marked is the transition between upper reaches that drain 1e^5 - 1e^7 m^2 (red line) and lower reaches that drain 1e^7 - 1e^{10} m^2 (cyan line), with relative k_s, θ, k_{sn} (for $\theta_{ref} = 0.39$) and R^2.

Figure S2: Result from the variance minimization method used to calculate $\theta_{ref} = 0.41$ for the eastern Rockies drainage network (TopoToolbox v2; Schwanghart and Scherler, 2014).

Figure S3: Flexural response of the Arkansas River valley across the western High Plains under T_e = 5, 10, and 15 km. The flexural load is calculated from an inferred eroded volume based on remnants of the oldest terrace in the western High Plains, the Rocky Flats (~1.3-2 Ma) (red polygons in Fig. 1, main text).

Table S1: Summary of terrace strath elevations and alluvial fill thicknesses as measured in the field (Figure 7, main text). Terrace names are after Scott et al. (1972, 1977).

References

Berlin, M.M., and Anderson, R.S., 2007, Modeling of knickpoint retreat on the Roan Plateau, western Colorado: Journal of Geophysical Research, v. 112, p. F03S06, doi:10.1029/2006JF000553.

Crosby, B.T., and Whipple, K.X., 2004, Knickpoint initiation and distribution within fluvial networks: 236 waterfalls in the Waipaoa River, North Island, New Zealand: Geomorphology, v. 82, p. 16–38, doi:10.1016/j.geomorph.2005.08.023.

Gallen, S.F., 2018, Lithologic controls on landscape dynamics and aquatic species evolution in post-orogenic mountains: Earth and Planetary Science Letters, v. 493, p. 150–160, doi:10.1016/j.epsl.2018.04.029.

Gallen, S.F., Wegmann, K.W., and Bohnenstiehl, D.W.R., 2013, Miocene rejuvenation of topographic relief in the southern Appalachians: GSA Today, v. 23, p. 4–10, doi:10.1130/GSATG163A.1.

Goren, L., Willett, S.D., Herman, F., and Braun, J., 2014, Coupled numerical-analytical approach to landscape evolution modeling: Earth Surface Processes and Landforms, v. 39, p. 522–545, doi:10.1002/esp.3514.

Hansen, S.M., Dueker, K.G., Stachnik, J.C., Aster, R.C., and Karlstrom, K.E., 2013, A rootless Rockies-support and lithospheric structure of the Colorado Rocky Mountains inferred from CREST and TA seismic data: CREST: Geochemistry, Geophysics, Geosystems, v. 14, p. 2670–2695, doi:10.1002/ggge.20143.

Kirby, E., and Whipple, K.X., 2012a, Expression of active tectonics in erosional landscapes: Journal of Structural Geology, v. 44, p. 54–75, doi:10.1016/j.jsg.2012.07.009.

Kirby, E., and Whipple, K.X., 2012b, Expression of active tectonics in erosional landscapes: Journal of Structural Geology, v. 44, p. 54–75, doi:10.1016/j.jsg.2012.07.009.

Lazear, G., Karlstrom, K., Aslan, A., and Kelley, S., 2013, Denudation and flexural isostatic response of the colorado plateau and southern rocky mountains region since 10 Ma: Geosphere, v. 9, p. 792–814, doi:10.1130/GES00836.1.

Miller, S.R., Sak, P.B., Kirby, E., and Bierman, P.R., 2013, Neogene rejuvenation of central Appalachian topography: Evidence for differential rock uplift from stream profiles and erosion rates: Earth and Planetary Science Letters, v. 369–370, p. 1–12, doi:10.1016/j.epsl.2013.04.007.

Schwanghart, W., and Scherler, D., 2014, Short Communication: TopoToolbox 2 – MATLAB-based software for topographic analysis and modeling in Earth surface sciences: Earth Surface Dynamics, v. 2, p. 1–7, doi:10.5194/esurf-2-1-2014.

Scott, G.R., 1977, Reconnaissance geologic map of the Cañon City Quadrangle, Fremont County, Colorado: USGS Miscellaneous Field Studies Map Geological maps.

Scott, G.R., 1972, Reconnaissance geologic map of the Hobson quadrangle, Pueblo and Fremont County, Colorado: USGS.

Snyder, N.P., Whipple, K.X., Tucker, G.E., and Merritts, D.J., 2000, Landscape response to tectonic forcing: Digital elevation model analysis of stream profiles in the Mendocino triple junction region, northern California: Geological Society of America Bulletin, v. 112, p. 1250–1263.

Watts, A.B., 2001, Isostasy and flexure of the lithosphere: Cambridge ; New York, Cambridge University Press, 458 p.

Wobus, C., Whipple, K.X., Kirby, E., Snyder, N., Johnson, J., Spyropolou, K., Crosby, B., and Sheehan, D., 2006, Tectonics from topography: Procedures, promise, and pitfalls, *in* Tectonics, Climate, and Landscape Evolution, Geological Society of America, doi:10.1130/2006.2398(04).

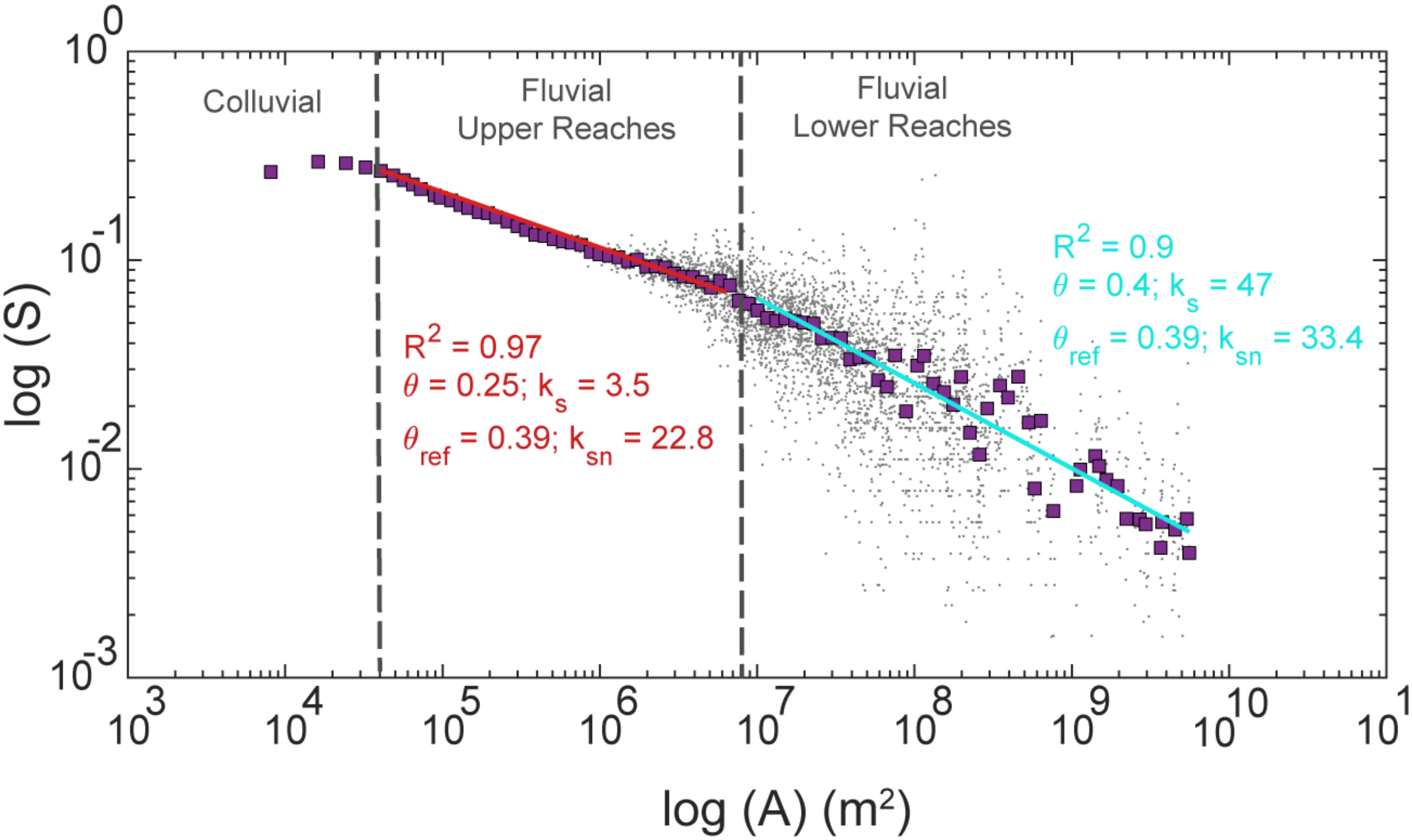

Colluvial
Fluvial
Upper Reaches
Fluvial
Lower Reaches
R^2 = 0.97
θ = 0.25; k_s = 3.5
θ_{ref} = 0.39; k_{sn} = 22.8
R^2 = 0.9
θ = 0.4; k_s = 47
θ_{ref} = 0.39; k_{sn} = 33.4
log (S)
log (A) (m^2)
10^0
10^{-1}
10^{-2}
10^{-3}
10^3
10^4
10^5
10^6
10^7
10^8
10^9
10^{10}
10^{11}

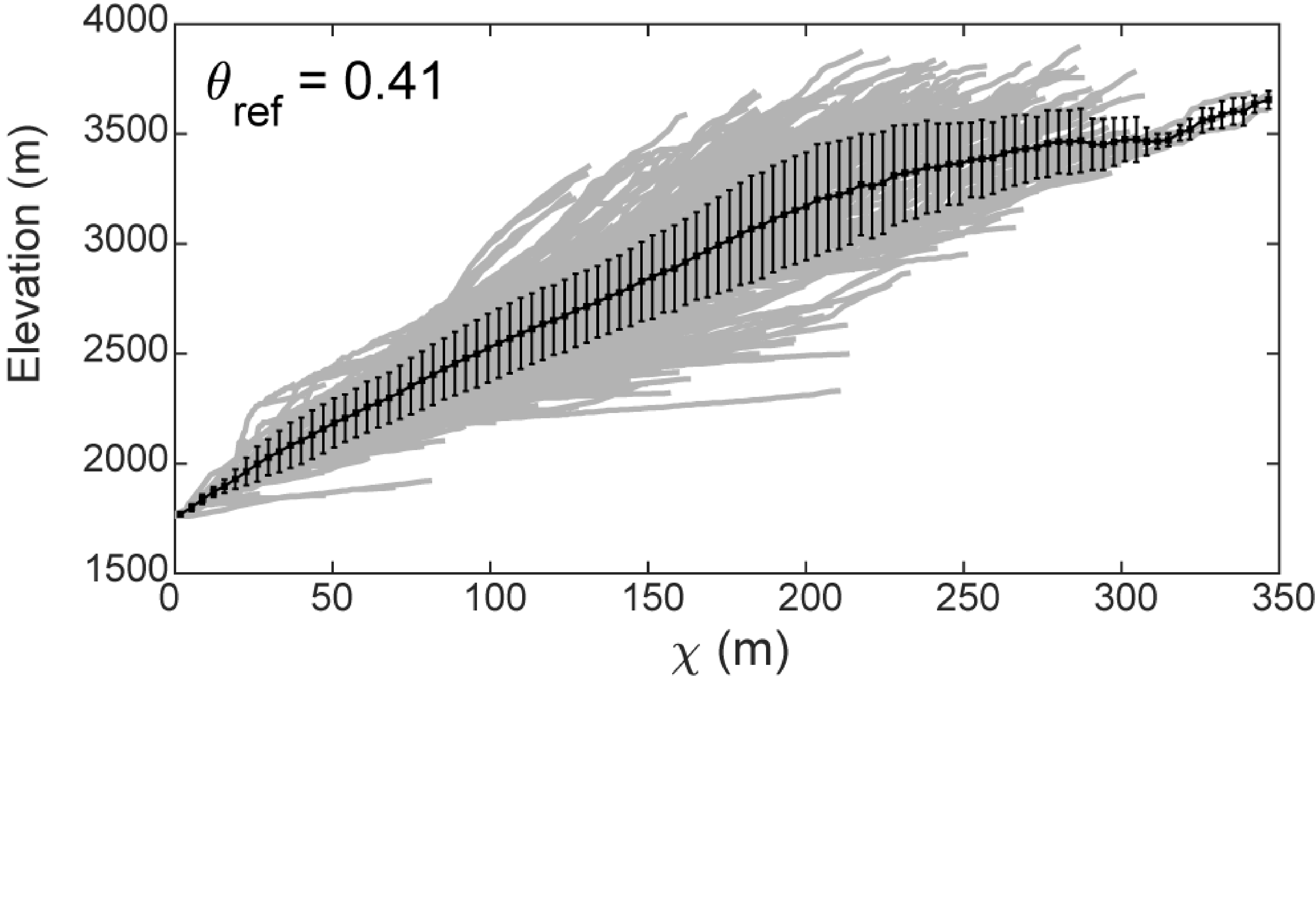

θ_{ref} = 0.41
Elevation (m)
4000
3500
3000
2500
2000
1500
0
50
100
150
200
250
300
350
χ (m)

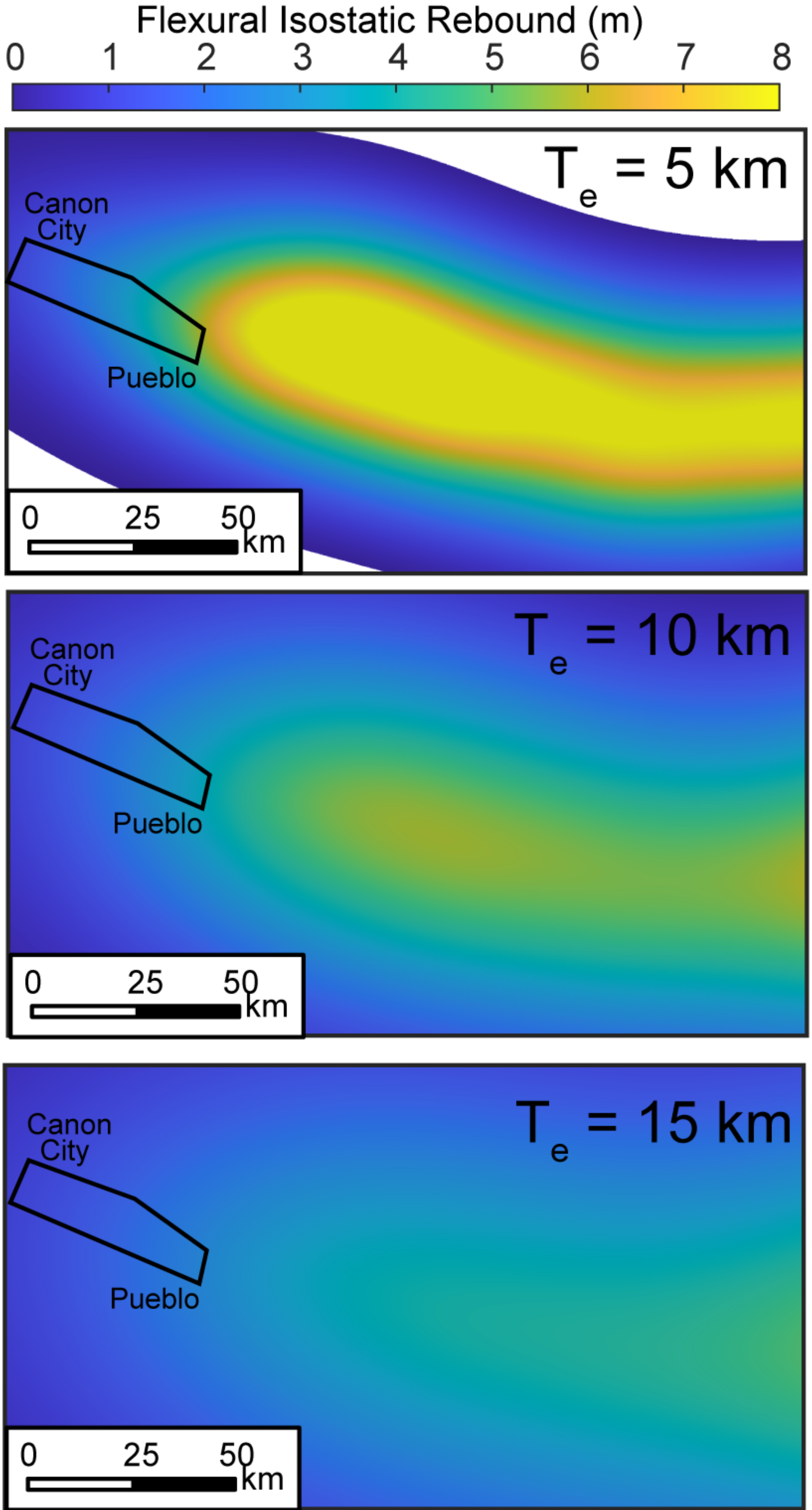

Flexural Isostatic Rebound (m)
0
1
2
3
4
5
6
7
8
T_e = 5 km
Canon City
Pueblo
0
25
50
km
T_e = 10 km
Canon City
Pueblo
0
25
50
km
T_e = 15 km
Canon City
Pueblo
0
25
50
km